

EMF Exposure Mitigation in RIS-Assisted Multi-Beam Communications

Herman L. dos Santos*, Cristian J. Vaca-Rubio[†], Radosław Kotaba[†], Yi Song[‡],
Taufik Abrão*, and Petar Popovski[†]

**Department of Electrical Engineering, Universidade Estadual de Londrina, Londrina, Brazil*

[†]*Department of Electronic Systems, Aalborg University, Aalborg, Denmark*

[‡]*School of Electrical and Information Engineering, Zhengzhou University, Zhengzhou, China*

E-mail: hermanlds@gmail.com, {civr, rak, petarp}@es.aau.dk, songyizzu@gs.zzu.edu.cn, and taufik@uel.br

Abstract—This paper proposes a method for reducing third-party exposure to electromagnetic fields (EMF) by exploiting the capability of a reconfigurable intelligent surfaces' (RIS) to manipulate the electromagnetic environment. We consider users capable of multi-beam communication, such that a user can use a set of different propagation paths enabled by the RIS. The optimization objective is to find propagation alternatives that allow to maintain the target quality of service while minimizing the level of EMF at surrounding non-intended users (NUEs). We provide an evolutionary heuristic solution based on Genetic Algorithm (GA) for power equalization and multi-beam selection of a codebook at the Base Station. Our results show valuable insights into how RIS-assisted multi-beam communications can mitigate EMF exposure with minimal degradation of the spectral efficiency.

Index Terms—Electromagnetic Field Exposure, Reconfigurable Intelligent Surfaces, Multi-Beam Communications.

I. INTRODUCTION

The rapid increase of the number of connected devices raises concerns about the EMF exposure (EMFE) from the signaling of devices under these technologies [1]. As the 6th-Generation (6G) moves towards providing sustainable wireless connectivity, it is imperative to explore innovative approaches to control EMFE [2].

Recent literature features several methods to deal with the EMFE concern [3]–[7]. One promising direction for EMFE-aware communications in 6G systems relies on the concept of reflective intelligent surface (RIS), which consists of electronically controlled reflective elements that can passively perform signal phase-shifting. In this way, RIS acts as a system element that can manipulate the electromagnetic environment [5]. Some studies include RIS-assisted resource allocation (RA) in EMFE-aware communications [4], [6], [7].

Uplink (UL) EMFE-aware communications in RIS-assisted scenario have been studied in [4]. The authors state that the users' equipment (UEs) are very exposed

This work was supported in part by the Coordenação de Aperfeiçoamento de Pessoal de Nível Superior - Brasil (CAPES) – Finance Code 001 and by the National Council for Scientific and Technological Development (CNPq) of Brazil under Grants 405301/2021-9, 141485/2020-5, and 310681/2019-7. R. Kotaba and P. Popovski were supported in part by the H2020 RISE-6G project financed by the European Commission under grant no. 101017011. P. Popovski was supported by the Villum Investigator Grant “WATER” from the Velux Foundation. C. J. Vaca-Rubio was supported by the European Union's Horizon EUROPE research and innovation program under grant agreement No. 101037090 - project CENTRIC.

in UL transmissions and propose a scenario exploiting the RIS reflective capabilities to increase the signal power received at the base station (BS). By jointly optimizing the combiner beamforming (BF) vector, RIS coefficients, and transmit power, it is possible to significantly reduce the EMFE. Furthermore, the RIS can provide energy-efficient EMFE-aware communications [6] in UL multi-antenna scenarios. It is shown that using the RIS it is possible to surpass the EMFE constraint and maintain fairly the energy efficiency.

Besides self-EMFE-aware communications, in a real-world environment the UL or downlink (DL) communication from a UE might affect its surrounding in the sense of exposing other people to EMF radiation. We use the term non-intended UE (NUE) to denote those people, as they are potential users of the communication system at a future instant, but presently not communicating with the BS. The millimeter-wave (mmWave) have been employed in this scenario [7]. The orthogonality provided by the small wavelength turn possible transmitting in a two-path manner, BS-UE and BS-RIS-UE, and the authors show that it is possible to maximize the spectral efficiency (SE) of a user when the direct path is constricted by the presence of a NUE. However, the method depends on high signaling overhead, *e.g.* channel estimation (CHEST) to both UE and NUE, and may be sensitive when the low-exposure constraint appears in both paths. Moreover, CHEST routine can provide environment mapping [8], being able to localize the NUEs as scatterers, reducing the exposure and overhead of estimating the channel of these users.

Contributions: In this work, we address the problem of EMFE-aware communications by exploiting multi-beam communication to compose the BF vector, thereby providing an effective solution for EMFE mitigation under requirements of SE. The solution is obtained via evolutionary heuristic techniques, namely Genetic Algorithm (GA). The results are evaluated for two scenarios: a) with perfect channel state information (CSI); and b) scenario with only the localization information is available. The method is able to keep track of the EMFE under both assumptions.

II. SYSTEM MODEL

Consider a mmWave time division duplex (TDD) multiple-input, multiple-output (MIMO) system where a BS equipped with M antennas communicates in DL with

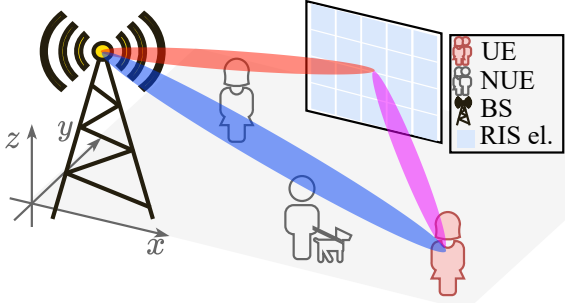


Figure 1. mmWave multi-beam EMFE-aware DL system.

a single-antenna UE aided by an RIS composed of N reflective elements. Both BS antennas and RIS elements are arranged in a rectangular uniform linear array (ULA) fashion with $d = \lambda/2$ meters spacing, where λ is the carrier wavelength. The elements are positioned such that the normal of BS antennas is aligned with the x -axis, *i.e.* $M_y = M_z$, and RIS elements are distributed with $N_x = N_z$. The BS communicates with the UE using a BF vector:

$$\mathbf{w} = \sum_{m=1}^M \sqrt{\rho_m} \mathbf{w}_m \in \mathcal{C}^{M \times 1} \quad (1)$$

where $\mathbf{W} = [\mathbf{w}_1, \mathbf{w}_2, \dots, \mathbf{w}_M] \in \mathcal{C}^{M \times M}$ is the codebook and $\boldsymbol{\rho}$ the power allocation (PA) vector. A representation of the system is depicted in Fig. 1. In such a case, the BS can choose to exploit the direct, reflected paths, or multiple beams to compose the signal. The DL transmitted symbol y is represented as

$$\mathbf{y} = \mathbf{w}^H x = \left(\sum_{m=1}^M \sqrt{\rho_m} \mathbf{w}_m^H \right) x \in \mathcal{C}^{M \times 1} \quad (2)$$

where x is the transmitted complex symbol, which has unitary power, *i.e.*, $\mathbb{E}[|x|^2] = 1$ and $[\cdot]^H$ denotes the Hermitian transpose operator. The *reciprocal channel* of the k -th UE is composed by the reflected and direct paths:

$$\mathbf{h}_k = \underbrace{\mathbf{H}_B^{RH} \boldsymbol{\Phi} \mathbf{h}_R^k}_{\text{reflected path}} + \underbrace{\mathbf{h}_B^k}_{\text{direct path}}, \quad (3)$$

where $\mathbf{H}_B^R \in \mathcal{C}^{N \times M}$ is the BS-RIS channel, $\mathbf{h}_R^k \in \mathcal{C}^{N \times 1}$ and $\mathbf{h}_B^k \in \mathcal{C}^{M \times 1}$ are the RIS-UE and BS-UE channel vectors, respectively. The matrix $\boldsymbol{\Phi} = \text{diag}(\boldsymbol{\phi}) \in \mathcal{C}^{N \times N}$ is a diagonal matrix of RIS elements phase-shift, and $\phi_{i,i} = e^{j\phi_i} \in [-\pi; \pi]$ denotes the i -th diagonal entry. Along with the active UE, there is a set of NUEs that are not communicating with the BS and *should not be exposed to excessive* electromagnetic field (EMF). The EMFE is defined as the power density that impinges in a specific area, which is discussed further in this paper. The channel BS-NUEs follows the same rule as applied to UE.

We adopt the Rayleigh channel model [9] with the channels coefficients described as a factor of the path-loss (PL), specifically mmMAGIC urban line-of-sight (LoS) model [10], Eq. (4), and small-scale fading configuring multi-path propagation. The PL is dependent of three-dimensional (3D) Euclidean distance d_{3D} in meters, the carrier frequency f_c in GHz, and stochastic shadow fading standard deviation σ_{SF} in dB:

$$\beta = 19.2 \log_{10}(d_{3D}) + 32.9 + 20.8 \log_{10}(f_c) + \sigma_{\text{SF}}. \quad (4)$$

This PL model is valid for the range of 6 to 100 GHz and assumes LoS propagation. Hence, the channel is a product of the PL with random amplitudes and phases normally distributed, unitary variance, from small-scale fading modeling. We evaluate the signal power impinging in an arbitrary point in space $\mathbf{q} \in \mathbb{R}^{3 \times 1}$ as¹

$$|\mathbf{y}_q|^2 = |\mathbf{w}^H (\mathbf{H}_B^{RH} \boldsymbol{\Phi} \mathbf{h}_R^q + \mathbf{h}_B^q)|^2. \quad (5)$$

III. EMFE-AWARE COMMUNICATIONS

The objective of our design is twofold. We would like to increase, or at least maintain the quality of service for the UE, while limiting the EMFE at points/areas where the NUEs are located. This is achieved by considering multiple propagation paths (besides the direct and reflected paths), which offers a bigger solution space. For the sake of tractability, we focus on the designs exploiting mutually orthogonal beams, *i.e.* not interfering with each other, which further allows us to apply power equalization along with beam selection. Throughout, we assume the NUEs' positions are known.²

A. Codebook design and Spectral Efficiency

The ability to manipulate the electromagnetic environment with RIS adds another degree of freedom to communication systems. Because the reflected path can be controlled, it becomes a viable solution for EMFE constrained communications [7], in addition to the direct path between BS and UE. To that end, in this work we examine both *direct and reflected paths* while taking into account a *threshold for the power allocated to the direct one*. This threshold is determined using maximum ratio transmission (MRT) and is necessary due to the presence of the NUE between the BS and UE. The remaining power is then allocated to the reflected path. However, such an approach is very sensitive to the quality of the CHEST routine. To overcome this issue, we choose a discrete Fourier transform (DFT) codebook-based approach, defining a *set of orthogonal beams* obtained by the DFT used to communicate with the UE. The codebook of orthogonal codewords used by both BS and RIS is defined as:

$$\mathbf{W}^I = \{\boldsymbol{\mu}_i\}_{i=1}^{\sqrt{I}} \otimes \{\boldsymbol{\nu}_j\}_{j=1}^{\sqrt{I}}, \quad (6)$$

with $I \in \{N, M\}$ and

$$\boldsymbol{\mu}_i = \left[1, e^{\frac{2\pi(i-1)}{\sqrt{I}}}, \dots, e^{\frac{2\pi(i-1)(\sqrt{I}-1)}{\sqrt{I}}} \right], \quad (7)$$

$$\boldsymbol{\nu}_j = \left[1, e^{\frac{2\pi(j-1)}{\sqrt{I}}}, \dots, e^{\frac{2\pi(j-1)(\sqrt{I}-1)}{\sqrt{I}}} \right]. \quad (8)$$

where the operator \otimes is the Kronecker product.

Using Shannon's capacity equation [11], the UE SE is obtained by considering the ratio of impinging signal power, the receiver noise power σ_w^2 , and the bandwidth B , also considering BF vectors $\boldsymbol{\rho}$ as:

$$\text{SE} = B \log_2 \left(1 + \frac{|\mathbf{w}^H (\mathbf{H}_B^{RH} \boldsymbol{\Phi} \mathbf{h}_R^k + \mathbf{h}_B^k)|^2}{\sigma_w^2} \right), \quad (9)$$

¹A point \mathbf{q} may represent a UE, NUE, or compose a set denoting a group of NUEs.

²Localization methods are out of scope herein. Future works will encompass methods and performance under localization errors.

where $\sigma_w^2 = B \cdot N_0 \cdot N_f$, being N_0 the noise power spectral density and N_f the noise figure.

EMFE-aware optimization: The BS equalizes the power between the beams available in \mathbf{W} assigning values to ρ . The EMF manipulation is proportional to the power of the signal that impinges on the target points in set $\mathcal{Q} = \{q_1, q_2, \dots, q_{|\mathcal{Q}|}\}$, being $|\mathcal{Q}|$ the cardinality of the set. The problem is subject to a minimum SE to the UE. Hence, the power density \bar{P} in [W/m²] or [W/Area- \mathcal{Q}] over a specific area such that the sum of the power density in each point $q \in \mathcal{Q}$ can be expressed as:

$$\bar{P} = \frac{1}{|\mathcal{Q}|} \sum_{q \in \mathcal{Q}} \left| \mathbf{w}^H (\mathbf{H}_B^{RH} \Phi \mathbf{h}_R^q + \mathbf{h}_B^q) \right|^2. \quad (10)$$

We can formally describe the EMFE-aware communications as a minimization of power density \bar{P} over a set of points \mathcal{Q} , Eq. (10), under the EMFE and physical constraints of the system. This problem is formulated as

$$(\mathcal{P}1) \quad \underset{\rho, \phi}{\text{minimize}} \quad \bar{P} \quad (11a)$$

$$\text{s.t.} \quad \text{SE} \geq \text{SE}_{\min}, \quad (11b)$$

$$\mathbf{w} \in \mathbf{W}^B \quad (11c)$$

$$\phi \in \mathbf{W}^R \quad (11d)$$

$$\sum_{i=1}^M \rho_i \leq P \quad (11e)$$

wherein (11b) expresses the constraint of guaranteed SE to the UE, (11c) limits the BS BF vectors to concatenating the codebook words, while (11d) implies the usage of a vector in RIS codebook as reflection coefficients. Finally, (11e) formally delimits the power pool constraint. It is worth noting that ($\mathcal{P}1$) is challenging to solve due to the non-convexity of the objective function and constraints.

B. CHEST and Localization Impairments

The problem ($\mathcal{P}1$) can achieve global minima if the CSI have been perfectly estimated, which is a weak assumption since the CHEST process can be quite costly in terms of resources and signaling. An alternative solution, requiring less overhead, is the estimation of the positions of the environmental elements through sensing.

For CHEST routine, κM and κMN channel coefficients need to be estimated for direct and reflected paths, respectively, where $\kappa \triangleq K + \tilde{K}$ denotes K UEs and \tilde{K} NUEs. Based on the three-phase CHEST framework [12], the minimum signaling consisting of

$$\kappa + N + \max \{ \kappa - 1, \lceil (\kappa - 1) \cdot N/M \rceil \} \quad [\text{pilots}]$$

is necessary just for perfectly recovering CSI, and that is under the assumption of no receiver noise, which is unrealistic. Hence, perfect CSI is an idealized case but is employed to derive upper bounds of system performance.

In contrast to traditional RIS CHEST procedures that require the cascaded channel estimation at either the BS or the UE, several recent works use the localization of the UEs [13], [14] in joint sensing and communication (JSAC). JSAC allows retrieving environmental information along with the NUE position, which suits the case of EMFE mitigation since the same signaling used to localize

the UE of interest can be employed to retrieve the NUEs position. For instance, the proposed framework in [13] reduces pilot overhead and the need for frequent RIS reconfiguration by optimizing the configuration of the RIS for several channel coherence intervals. This leads to a novel frame structure, comprising infrequent localization and RIS control tasks, combined with a more frequent optimization of the BS precoders to maximize the transmission rate. This approach leverages accurate location information obtained with the aid of several RISs as well as novel RIS optimization and CHEST methods. These works further motivate our method, in which by obtaining the users' location, we can avoid the dense overhead related to the CHEST procedure.

IV. PROPOSED SOLUTIONS

We study and compare two approaches to solve the EMFE optimization problem; *a*) the rate maximization constrained by EMFE framework originally presented in [7], namely DFT-based beam and power optimization; *b*) employment of evolutionary heuristic, specifically GA, to exploit the solution space of combining more than two beams.

MRT and DFT beam (MRT-DFT) [7]: assuming perfect CSI of both UE and NUE, obtaining a quasi-optimal and low complexity solution. The method is set as follows. The direct beam, \mathbf{w}_d , follows a MRT rule, taking its' coefficients as the inverse of the direct BS-UE channel, and another jointly optimizes the BF vector towards the RIS and its' reflection coefficients by extracting the word with the maximum gain and matching the beam \mathbf{w}_r . Hence, the power of each beam is weighted to maximize the SE under a constraint of maximum impinging power at the NUE. We describe this implementation in Algorithm 1.

Algorithm 1 MRT and DFT beam [7]

Input: $\mathbf{W}^R, \mathbf{H}_B^R, \mathbf{h}_B^k, \mathbf{h}_R^k, \mathbf{h}_B^q, \mathbf{h}_R^q, P, \bar{P}$

Output: $\mathbf{w}_d, \mathbf{w}_r, \Phi, \rho_d, \rho_r$

- 1: Define $\mathbf{w}_d \leftarrow \mathbf{h}_B^k / \|\mathbf{h}_B^k\|$
 - 2: **for** $i = 1$ to N **do**
 - 3: $\Phi \leftarrow \text{diag}(\mathbf{W}_R^i)$
 - 4: Evaluate $|\mathbf{H}_B^{RH} \Phi \mathbf{h}_R^k|^2$
 - 5: Store the reflected path power gain under \mathbf{W}_R^i
 - 6: **end for**
 - 7: Assign the beam with the highest gain to Φ ;
 - 8: Define $\mathbf{w}_r^H \leftarrow (\mathbf{H}_B^{RH} \Phi \mathbf{h}_R^k)^H / \|\mathbf{H}_B^{RH} \Phi \mathbf{h}_R^k\|$
 - 9: $\rho_d \leftarrow \bar{P} / \|\mathbf{w}_d^H \mathbf{h}_B^q\|$
 - 10: $\rho_r \leftarrow P - \rho_d$
-

The implementation presented in Algorithm 1 assumes perfect CSI for both UE and NUE. The performance and reliability are equivalent to the CHEST results. It is pointed out that another drawback is when both direct and reflected path is virtually obstructed let's say by NUEs, limiting the amount of power that can be employed. We choose to exploit such characteristics in our numerical results.

Multi-Beam Power Equalization by GA (MB-GA): we propose the use of a GA in M -beam search-and-weighting defined in codebook \mathbf{W}^B . We choose this method because the non-linear, non-convex, mixed integer-quadratic programming problem of $\mathcal{P}1$ is not solvable in a polynomial time, while GA has a widespread in the search space. Generally, this method attains at least quasi-optimal solutions when the problem is well-defined by a cost function. The authors highlight that there are several methods for solving ($\mathcal{P}1$), and will be investigated in future works. The GA procedure is performed as [15]:

1. Creating Initial Population: a number of initial population n_P of chromosomes $\mathcal{X}^0 = \{\mathbf{x}_1, \mathbf{x}_2, \dots, \mathbf{x}_{n_P}\}$, *i.e.* individual candidate solutions, Eq. (12), is uniformly generated in feasible solution space. We generate a batch of solutions under the constraints defined in equations (11d) and (11e), check their feasibility by evaluating Eq. (11b), and re-generate those that do not attend to the constraints. These entries are organized as

$$\mathbf{x}_i = [\rho_1, \rho_2, \dots, \rho_M, \boldsymbol{\omega}^R]^T, \quad i = \{1, 2, \dots, n_P\}, \quad (12)$$

being $\boldsymbol{\omega}^R \in \{0, 1\}^{N \times 1}$, $\sum \boldsymbol{\omega}^R = 1$, and $\Phi = \mathbf{W}^R \boldsymbol{\omega}^R$.

2. Scoring and Scaling of Population: the solutions are scored as their problem-specific fitness function, Eq. (10), value³ $\mathcal{Y}^j = f(\mathcal{X}^j)$, being j the generation index. Then, the solutions are escalated to ensure those with higher quality are most likely chosen as the next generation of parents. Formally, the escalated solution in j -th iteration is defined as

$$\bar{\mathcal{Y}}^j = g(\mathcal{Y}^j) = \alpha \mathcal{Y}^j \quad (13)$$

being α the scaling function, which is a design parameter.

3. Elite Retaining and Tournament: the elite count e_C parameter defines how many individuals are guaranteed to advance to the next generation after scaling. The e_C solutions with the lowest fitness function values are parents for the offspring. The rest of the parents are selected by a *tournament function*, which randomly selects n_T individuals, defining which *survives* by applying a probabilistic test. Formally, the probability of the k -th individual proceeding in the tournament is:

$$p_k = \frac{\bar{y}_k}{\sum_{i=1}^{n_T} \bar{y}_i}, \quad k \in n_T \quad (14)$$

where n_T is a parameter that defines how many individuals besides the elite are allowed in the next generation. The probability of an individual surviving a generation is proportional to the quality of its solution.

4. Crossover and Mutation: At the end of a generation, the crossover function is applied in the set of parents, including the elite and tournament winners, and the mutation function in the offspring generation. The n_T individuals left from elite count plus tournament result are input to the crossover function, which creates the children by combining the values of two solutions, let's say \mathbf{x}_i and \mathbf{x}_j , $\bar{y}_i < \bar{y}_j$, and multiplying by a random value. Formally, the child $\bar{\mathbf{x}}$ which belongs to the next generation is defined as

$$\bar{\mathbf{x}} = \mathbf{x}_i + \mathcal{U}[0, 1](\mathbf{x}_i - \mathbf{x}_j). \quad (15)$$

After defining the crossover, the *mutation* process is applied. The mutation occurs under a probability p_m , also

³As the GA is applied in the cost function minimization, the lower the value of the fitness function, the better is the candidate-solution.

a parameter of design, and replaces an entry of the child solution with a random value. The mutation defines the end of a generation, then the algorithm goes back to Step 2 and proceeds until a stopping criterion is satisfied.

V. SIMULATION RESULTS

We carry out Monte Carlo simulations (MCS) to evaluate and compare with the reference method [7], which assumes perfect knowledge of the CSI and does not exploit the sensing capabilities of RIS for location estimation. We evaluate the methods with one and two NUEs in four scenarios, as depicted in Figure 1, where the NUE₁ represents the one in BS-UE line (person with a dog, in the graphical representation), and NUE₂ in BS-RIS line. Four configurations are evaluated:

- Scenario 1.1: There is one NUE moving along the line between the BS and UE. We assume the BS, RIS, NUE and UE are all at the same height z .
- Scenario 1.2: There is one NUE moving along the line between the BS and UE. We assume the BS, RIS, NUE and UE where the different heights follow the rule $BS_z > RIS_z > UE_z = NUE_z$.
- Scenario 2.1: There are two NUEs moving along the line between the BS and UE, and the line between the BS and RIS. We assume the BS, RIS, NUE and UE are all at the same height z .
- Scenario 2.2: There are two NUEs moving along the line between the BS and UE, and the line between the BS and RIS. We assume the BS, RIS, NUE and UE with different heights following the rule $BS_z > RIS_z > UE_z = NUE_z$.

Scenarios 2.1/2.2 are more challenging due to the limitation in the amount of power that can be allocated to the direct path. To ensure a fair comparison, we set SE_{\min} equals to the SE obtained in DFT-based BF scheme. For both methods, we consider the selected beams leak some energy, which increases the evaluated exposure and SE. We will evaluate the results under two use cases *i*) the ideal assumption of perfect knowledge of the CSI, and *ii*) the estimation via the UEs and NUEs locations. We detail the parameters of our simulation in Table I.

A. Performance under Perfect CSI

Here we evaluate the performance of the method with perfect CSI information for the described scenarios.

Scenarios 1.1 and 1.2: Scenario 1 represents straightforward the baseline scenario. There is only NUE₁ performing *virtual* blockage in the direct path. Intuitively, this scenario is the one that brings the performance upper bound in terms of achievable SE since the reflected path can be fully exploited. The performance under perfect CSI for both methods is presented in Fig. 2.

Fig. 2 shows that the larger search space provided in our proposal (solid lines) is capable of improving the SE while achieving low exposure communication. For both methods, we evaluated the performance considering the instantaneous coefficients of the channels were known to the BS. Exploiting the higher search space reveals that our method can compose a multi-beam transmission

Table I
SIMULATION PARAMETERS

System		
Parameter	Value	
BS Ant.	36	
RIS El.	100	
BS Pos.	I. $[-80, 0, 1.5]$	[m]
	II. $[-80, 0, 10]$	[m]
RIS Pos.	I $[0, 50, 1.5]$	[m]
	II. $[0, 50, 5]$	[m]
UE Pos.	$[80, 0, 1.5]$	[m]
Carrier freq.	$f_c = 28$	[GHz]
Noise power	$N_0 = -174$	[dBm/Hz]
Noise figure	$N_f = 10$	[dB]
Bandwidth	$B = 100$	[MHz]
Available power	$P = 43$	[dBm]
Shadow Fading	$\sigma_{SF} = 2$	[dB]
Genetic Algorithm		
Population size	$nP = 300$	
Elite counter	$eC = 2$	
Tournament size	$nT = 4$	
Scaling function	α rank based	
Mutation probability	$p_m = 0.05$	
Constraints tolerance	10^{-6}	
Realizations	1000	MCS

coherently sums to the UE channel, surpassing the MRT-DFT method. Besides improving the rate of the UE, the composition of beams also can mitigate more efficiently the EMF, being more effective. The reference method utilizes all the power pool, *i.e.*, $\rho_d + \rho_r = P$, while the proposed method uses 0.79% of the available power, presenting an improvement in power allocation.

Scenarios 2.1 and 2.2: in these scenarios, the amount of power to be allocated is restricted in the both direct and reflected path since the EMFE constraint applies in both links. For the reference method, we apply the same rule of Algorithm 1 line 9 to the reflected path. Hence, the amount of power impinging in both NUES is trackable. The results obtained for both scenarios are depicted in Fig. 3. It shows a more significant performance gap in terms of rate. Both configurations of positioning, considering BS, RIS, NUE, UE with equal or different heights, achieved similar performances in terms of SE; however, the difference between the methods becomes clear. Compared to scenarios 1.1 and 1.2, the more truncated scenario highly

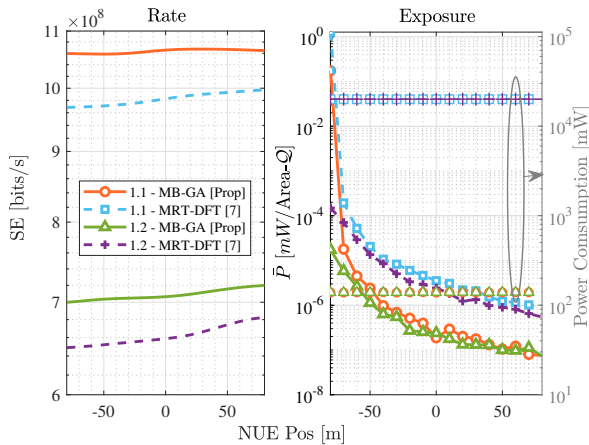


Figure 2. Achieved rate (*left*) and exposure (*right*) performance under perfect CSI for Scenario 1.1 and 1.2. The NUE is positioned in the origin of the y -axis and moves from -80 meters (BS position) to 80 meters (UE position).

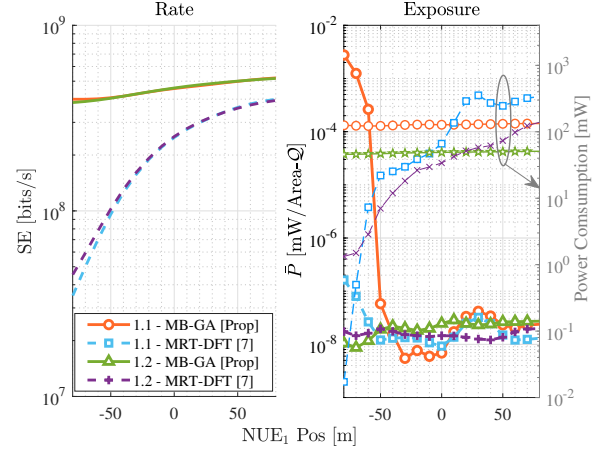


Figure 3. Achieved rate (*left*) and exposure (*right*) performance under perfect CSI for both scenarios 2.1 and 2.2. The NUE_1 has the same positioning as in scenarios 1.1 and 1.2, and NUE_2 is positioned in BS-RIS in steps of 5.494 meters.

limits the power, showing that the maximum achievable SE is half the value obtained earlier for the best case. The exposure of our method is higher, but the higher SE shows it is possible to manipulate the PA vector further to reduce the exposure at the cost of some rate degradation. Also, both methods are able to compensate for the higher path-loss in 3D scenarios since the used power is very limited, up to only 0.3 W for both methods. Due to the intrinsic characteristics of mmWave MIMO systems, this ends up being a more energy-efficient transmission.

B. Performance under Position Information

Here we evaluate the performance of the scenarios with limited information. Our goal is to check whether having only information about the position of the UE and NUES⁴ impacts communication and EMFE. In Section III-B we highlighted some drawbacks of using CSI, namely the overhead and self-exposure due to the CHEST procedure necessary for both UE and NUES. To that end, we present here the results assuming the BS has only the knowledge of NUES and UEs positions, *i.e.* the array response of the users. The methods applied by the BS are the same, but instead of using the channel vectors, the BS computes a geometrical channel based on the positions of two arbitrary elements [16]. While a degradation in the performance is expected since the BS is not aware of the multipath components that compose the channel coefficients, there is a benefit in avoiding CHEST procedure.

Scenarios 1.1 and 1.2: We again establish the baseline for our solution with simpler configurations. The results for this setup are presented in Fig. 4. As opposed to the perfect CSI case, our approach yields a lower rate when compared to the reference method. However, this cost is offset by a remarkable reduction in the EMF. Even when comparing the exposure levels with those achieved with perfect CSI, our method performs similarly and outperforms the reference approach. We would like to remark our approach prioritizes the reduction in EMF.

⁴We assume the BS obtains this information via a sensing phase. The exact procedure is out of the scope of this paper and is left for future work.

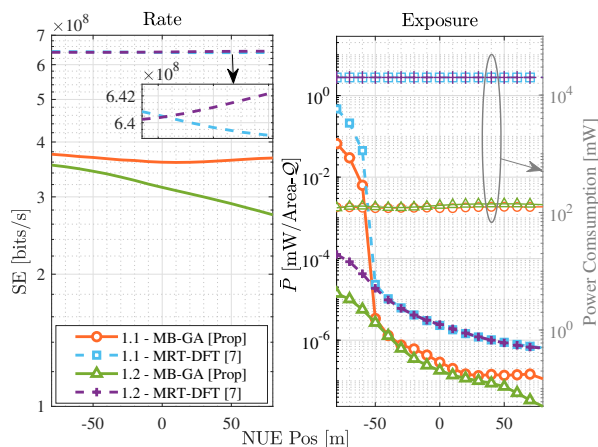


Figure 4. Achieved rate (left) and exposure (right) performance under localization for 1.1 and 1.2. The NUE is positioned in the origin of y -axis and move from -80 meters (BS position) to 80 meters (UE position).

Scenarios 2.1 and 2.2: When compared to the perfect CSI case, Fig. 5 reveals a similar rate performance between the two EMF mitigation methods, which can be attributed to the refined power control attained in MRT-DFT as it accounts for the specific channel coefficients, while the MB-GA is able to combine specific BF vectors that sum non-coherently with small scale coefficients of the NUEs, enabling the use of more power to the transmission. In Scenario 2.1, the EMFE levels appear to be similar to those of referenced method. However, in the most realistic Scenario 2.2, the proposed methods can attain substantial exposure reductions of up to two orders of magnitude w.r.t. [7]. Importantly, our approach consistently delivers higher ratios of obtained rate to exposure in $\frac{\text{bits/s}}{\text{mW/m}^2}$ across all scenarios, irrespective of the perfect CSI or localization approaches. This underscores the efficacy of our solution even under the most challenging conditions.

VI. CONCLUSION AND FUTURE WORKS

This work assessed the potential of multi-beam transmission with mmWave directivity and RIS multi-path enhancement. Our results reveal that, thanks to the physical characteristics of next-generation technologies, it is possible to exploit multiple propagation paths to improve the quality of service and reduce EMFE. Specifically, assuming perfect CSI, the MB-GA method overcomes another proposal in every metric at a complexity cost while assuming localization it has degraded SE performance but with lesser exposure. Future works include accounting for imperfect channel estimation and localization, as well as developing new algorithms to perform beam weighting.

REFERENCES

- [1] L. Chiaraviglio *et al.*, “Health Risks Associated With 5G Exposure: A View From the Communications Engineering Perspective,” *IEEE Open Journal of the Communications Society*, vol. 2, pp. 2131–2179, Aug. 2021.
- [2] F. E. Airod *et al.*, “Blue Communications for Edge Computing: the Reconfigurable Intelligent Surfaces Opportunity,” in *GLOBECOM 2022 - 2022 IEEE Global Communications Conference*, 2022, pp. 6396–6401.
- [3] D.-T. Phan-Huy *et al.*, “Creating and Operating Areas With Reduced Electromagnetic Field Exposure Thanks to Reconfigurable Intelligent Surfaces,” in *2022 IEEE 23rd International Workshop on Signal Processing Advances in Wireless Communication (SPAWC)*, Jul. 2022, pp. 1–5.

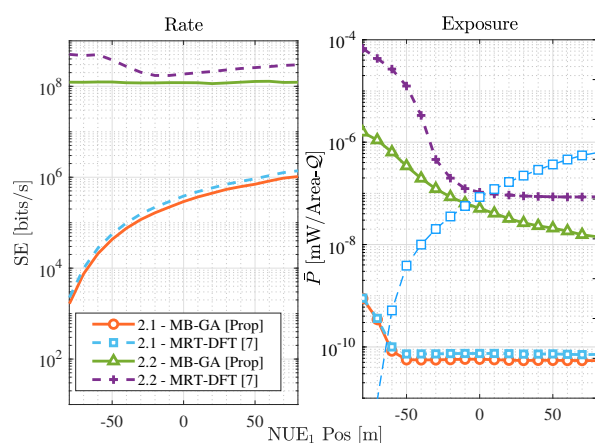


Figure 5. Achieved rate (left) and exposure (right) performance under localization for 2.1 and 2.2. The NUE₁ has the same positioning as in scenarios 1.1 and 1.2, and NUE₂ is positioned in BS-RIS in steps of 5.494 meters.

- [4] H. Ibraiwish, A. Elzanaty, Y. H. Al-Badarneh, and M.-S. Alouini, “EMF-Aware Cellular Networks in RIS-Assisted Environments,” *IEEE Communications Letters*, vol. 26, no. 1, pp. 123–127, Jan. 2022.
- [5] E. Björnson *et al.*, “Reconfigurable Intelligent Surfaces: A signal processing perspective with wireless applications,” *IEEE Signal Processing Magazine*, vol. 39, no. 2, pp. 135–158, Feb. 2022.
- [6] A. Zappone and M. D. Renzo, “Energy Efficiency Optimization of Reconfigurable Intelligent Surfaces With Electromagnetic Field Exposure Constraints,” *IEEE Signal Processing Letters*, vol. 29, pp. 1447–1451, Jun. 2022.
- [7] H. Guo *et al.*, “Electromagnetic Field Exposure Avoidance Thanks to Non-Intended User Equipment and RIS,” pp. 1537–1542, Dec. 2022.
- [8] Y. Lin *et al.*, “Channel Estimation and User Localization for IRS-Assisted MIMO-OFDM Systems,” *IEEE Transactions on Wireless Communications*, vol. 21, no. 4, pp. 2320–2335, 2022.
- [9] A. Goldsmith, *Wireless Communications*. Cambridge University Press, 2005.
- [10] T. S. Rappaport *et al.*, “Overview of Millimeter Wave Communications for Fifth-Generation (5G) Wireless Networks—With a Focus on Propagation Models,” *IEEE Transactions on Antennas and Propagation*, vol. 65, no. 12, pp. 6213–6230, Aug. 2017.
- [11] T. L. Marzetta *et al.*, *Fundamentals of Massive MIMO*. Cambridge University Press, 2016.
- [12] Z. Wang *et al.*, “Channel Estimation for Intelligent Reflecting Surface Assisted Multiuser Communications: Framework, Algorithms, and Analysis,” *IEEE Transactions on Wireless Communications*, vol. 19, no. 10, pp. 6607–6620, Jun. 2020.
- [13] F. Jiang and oterhs, “Optimization of RIS-Aided Integrated Localization and Communication,” *arXiv preprint arXiv:2209.02828*, 2022.
- [14] K. Keykhosravi *et al.*, “Leveraging RIS-Enabled Smart Signal Propagation for Solving Infeasible Localization Problems,” *arXiv preprint arXiv:2204.11538*, 2022.
- [15] V. D. P. Souto *et al.*, “A Novel Efficient Initial Access Method for 5G Millimeter Wave Communications Using Genetic Algorithm,” *IEEE Transactions on Vehicular Technology*, vol. 68, no. 10, pp. 9908–9919, 2019.
- [16] A. Albanese *et al.*, “MARISA: A Self-configuring Metasurfaces Absorption and Reflection Solution Towards 6G,” in *IEEE INFOCOM 2022 - IEEE Conference on Computer Communications*, 2022, pp. 250–259.